Inorg. Chem. **2009**, *48*, 2260−2268

Concerted Dismutation of Chlorite Ion: Water-Soluble Iron-Porphyrins As First Generation Model Complexes for Chlorite Dismutase

Michael J. Zdilla, Amanda Q. Lee, and Mahdi M. Abu-Omar*

Brown Laboratory, Department of Chemistry, Purdue University, 560 Oval Drive, West Lafayette, Indiana 47907

Received September 1, 2008

Three iron-5,10,15,20-tetraarylporphyrins (Fe(Por-Ar_4), Ar = 2,3,5,6-tetrafluro-*N,N,N*-trimethylanilinium (**1**), *N,N,N*-trimethylanilinium (**2**), and *p*-sulfonatophenyl (**3**)) have been investigated as catalysts for the dismutation of chlorite (ClO_2^-). Degradation of ClO_2^- by these catalysts occurs by two concurrent pathways. One leads to formation of chlorate (ClO_3^-) and chloride (Cl^-), which is determined to be catalyzed by O=Fe^{IV}(Por) (Compound II) based on stopped-flow absorption spectroscopy, competition with 2,2′-Azino-bis(3-ethylbenzothiazoline-6-sulfonicacid), ^{18}O-labeling studies, and kinetics. The second pathway is a concerted dismutation of chlorite to dioxygen (O_2) and chloride. On the basis of isotope labeling studies using a residual gas analyzer, the mechanism is determined to be formation of O=Fe^{IV}(Por)$^{\cdot+}$ (Compound I) from oxygen atom transfer, and subsequent rebound with the resulting hypochlorite ion (ClO^-) to give dioxygen and chloride. While the chlorate production pathway is dominant for catalysts **2** and **3**, the O_2-producing pathway is significant for catalyst **1**. In addition to chlorite dismutation, complex **1** catalyzes hypochlorite disproportionation to chloride and dioxygen quantitatively.

Introduction

The removal of toxic oxychlorine species (ClO_x^-) from drinking water is a problem that has garnered much attention in recent years because of the accumulation of these species as a result of their wide use as bleaching agents,[1] explosives,[2] herbicides,[3] and disinfectants.[4] Chlorite has been listed by the EPA as regulated toxic substance,[5a] and perchlorate is currently under consideration[5b] by the agency because of links to disease[5] and acute toxicity toward aquatic microorganisms.[6] Given the environmental and health concerns regarding water contamination by oxychlorine species, a wealth of work has been performed on the redox and decomposition chemistry of chlorine species.[7−10]

Perchlorate respiring bacteria (PRB) offer an exciting prospect for bioremediation of oxychlorine species. PRB possess two enzymes that employ oxychlorine species as metabolic oxidants for respiration. The first of these enzymes, perchlorate reductase (PR),[11] catalyzes the reduction of perchlorate to chlorate, and chlorate to chlorite (eq 1). The second enzyme, chlorite dismutase (Cld),[12] catalyzes the dismutation of chlorite ion to innocuous chloride and dioxygen (eq 1).

* To whom correspondence should be addressed. E-mail: mabuomar@purdue.edu.

(1) (a) Axegård, P.; Gunnarsson, L.; Malmqvist, A. *Sv. Papperstidning* **1989**, *92*, 50. (b) Germgård, U.; Tder, A.; Tormund, D. *Pap. Puu.* **1981**, *63*, 127.
(2) Hogue, C. *Chem. Eng. News* **2003**, *81*, 127.
(3) Åslander, A. *J. Agric. Res.* **1928**, *36*, 915.
(4) Harman, D. C.; Frankenberger, W. T. J. *J. Environ. Qual.* **1999**, *28*, 1018.
(5) (a) USEPA. National Primary Drinking Water Regulations; Disinfectants and Disinfection Byproducts Notice of Data Availability; Proposed Rule. *Fed. Regist.* **1998**, *63*, 15674. (b) USEPA. Priority List of Substances Which May Require Regulation under the Safe Drinking Water Act. *Fed.Regist* **1991**, *56*, 1470. (c) *Drinking Water and Health*; Boraks, J. , Ed.; National Research Council, National Academy Press: Washington, DC, 1987; pp 99−111.
(6) (a) Rosemarin, A.; Lehtinen, K-J.; Notini, M.; Mattsson, J. *Environ. Pollut.* **1994**, *85*, 3. (b) van Wijk, D. J.; Hutchingson, T. H. *Ecotoxicol. Environ. Safety* **1995**, *32*, 244. (c) Lehtinen, K-J.; Notini, M.; Mattsson, J.; Landner, L. *Ambio* **1998**, *17*, 387.
(7) For examples of iron-mediated chorite redox chemistry, see (a) Fábián, I. *Prog. Nucl. Energy* **2000**, *37*, 47. (b) Fábián, I.; Gordon, G. *Inorg. Chem.* **1992**, *31*, 2144. (c) Lednicky, L. A.; Stanbury, D. M. *J. Am. Chem. Soc.* **1983**, *105*, 3098. (d) Ondrus, M. G.; Gordon, G. *Inorg. Chem.* **1972**, *11*, 985. (e) Shakhashiri, B. Z.; Gordon, G. *J. Am. Chem. Soc.* **1969**, *91*, 1103. (f) Kahn, A. H.; Higginson, W. C. E. *J. Chem. Soc., Dalton Trans.* **1981**, 2537. (g) Birke, R. L., Jr *J. Am. Chem. Soc.* **1969**, *91*, 3481.
(8) For examples of iron-catalyzed decomposition of chlorite, see (a) Launer, H. F.; Wilson, W. K.; Flynn, J. H. *J. Res. Nat. Bur. Stand.* **1953**, *51*, 237. (b) Launer, H. F.; Tomimatsu, Y. *J. Am. Chem. Soc.* **1954**, *76*, 2591. (c) Schmitz, H.; Rooze, H *Can. J. Chem.* **1985**, *63*, 975.

10.1021/ic801681n CCC: $40.75
Published on Web 01/12/2009

$$ClO_4^- \xrightarrow{PR} ClO_3^- \xrightarrow{PR} ClO_2^- \xrightarrow{Cld} O_2 + Cl^- \qquad (1)$$

This second enzyme, which is the focus of our study, is a homotetrameric heme b enzyme with a molecular weight of 113 kD. It has been assumed that the iron porphyrin (a common motif for biocatalyzed oxidation chemistry) is directly responsible for the dismutation chemistry.[13] While some activity measurements have been done on native and recombinant forms of Cld,[12] very little is known about the molecular mechanism.[12e,f]

Chlorite and chlorous acid (abbreviated Cl(III)) have been the focus of much research. Several research groups have addressed the mechanistic details of the metal-free decomposition of Cl(III).[9] The reaction chemistry of Cl(III) with transition-metal ions has been reviewed by Fábián,[14] and much of the work has focused on aqueous nonheme Fe species as redox agents[7] and catalysts for decomposition.[8] While a number of metal species are known to catalyze the formation of oxygen from hypochlorite (OCl^-),[10a−d] synthetic systems that evolve O_2 from ClO_2^- are rare. Collman and co-workers have recently reported on a manganese-porphyrin catalyst for alkane oxidation by ClO_2^- that evolves O_2 as a minor side reaction.[15] To our knowledge this is the only example of metal-catalyzed oxygen-evolving chlorite decomposition.

Iron porphyrins are ubiquitous in biology as redox agents. Cytochrome *c* employs an iron-porphyrin as the electron carrier in the electron transport chain, peroxidases facilitate the conversion of dangerous peroxides, and cytochrome P450 catalyzes oxygen atom transfer reactions for drug metabolism and biological detoxification.[16] The latter is of particular interest to our current discussion of Cld in that it activates molecular O_2 in the transfer of O-atoms to substrate. This can be viewed as the reverse of the Cld reaction, which involves dioxygen evolution from the substrate, ClO_2^-.

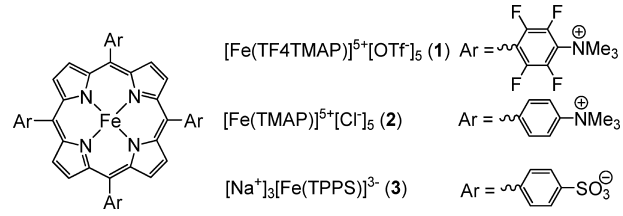

Figure 1. Water soluble iron porphyrins. TF_4TMAP = 5,10,15,20-tetrakis(2,3,5,6-tetrafluoro-4-*N,N,N*-trimethylanilinium)porhyrin; TMAP = 5,10,15,20-tetrakis(4-*N,N,N*-trimethylanilinium)porhyrin. TPPS = 5,10,15,20-tetrakis(4-sulfonatophenyl)porhyrin.

The traditional mechanism for cytochrome P450 implicates an oxoferryl porphryin radical cation species ($O{=}Fe^{IV}(Por)^{\bullet+}$, Compound I) as the oxygen transfer reagent.[17] However, recent results have implicated the involvement of more than one oxidizing species in cytochrome P450.[18,19] It remains to be seen what species are relevant to the mechanism of chlorite dismutase.

We have recently communicated the concerted dismutation of chlorite by an $Fe^{III}(TF_4TMAP)$ complex (TF_4TMAP = tetrakis(2,3,5,6-tetrafluro-*N,N,N*-trimethylanilinium)porphyrin).[20] In this work, we examine the full scope of this and several water-soluble iron porphyrins as biomimetic catalysts for Cld. Reaction kinetics, product distribution, ^{18}O-labeling studies, and competition with a sacrificial reductant (ABTS) are employed in determining operative mechanisms for the models and hence the enzyme.

Results

Evolution of O_2. We studied three water-soluble iron porphyrins (Fe(Por)) at neutral pH as model catalysts for Cld. These are shown in Figure 1. All three catalyze the degradation of ClO_2^- with formation of O_2 at varying efficiencies. Dioxygen evolution was monitored using an in-house built residual gas analyzer (RGA) consisting of a sample cell, the headspace of which is swept with an inert gas (usually nitrogen) which is carried to a single quadrupole

(9) For examples of metal-free decomposition of chlorite, see (a) Leitner, N. K.V.; Delaat, J.; Dore, M. *Water Res.* **1992**, *26*, 1655. (b) Deshwal, B. R.; Jo, H. D.; Lee, H. K. *Can. J. Chem. Eng.* **2004**, *82*, 619. (c) Cosson, H.; Ernst, W. R. *Ind. Eng. Chem. Res.* **1994**, *33*, 1468. (d) Jia, Z.; Margerum, D. W.; Francisco, J. S. *Inorg. Chem.* **2000**, *39*, 2614. (e) Furman, C. S.; Margerum, D. W. *Inorg. Chem.* **1998**, *37*, 4321.

(10) For examples of hypochlorite decomposition studies, see (a) Lister, M. W. *Can. J. Chem.* **1956**, *34*, 479. (b) Church, J. A. *Ind. Eng. Chem. Res.* **1994**, *33*, 239. (c) Ayres, G. H.; Booth, M. H. *J. Am. Chem. Soc.* **1955**, *77*, 825. (d) Ayres, G. H.; Booth, M. H. *J. Am. Chem. Soc.* **1955**, *77*, 828. (e) Adam, L. C.; Gordon, G. *Inorg. Chem.* **1999**, *38*, 1299. (f) Lister, M. W *Can. J. Chem.* **1956**, *34*, 479.

(11) Kengen, S. W. M; Rikken, G. B.; Hagen, W. R.; van Ginkel, C. G.; Stams, A. J. M. *J. Bacteriol.* **1999**, *181*, 6706. (b) Okeke, B. C.; Frankenberger, W. T. *Microbiol. Res.* **2003**, *158*, 337. (c) Bender, K. S.; Shang, C.; Cakraborty, R.; Belckik, S. M.; Coates, J. D.; Achenback, L. A. *J. Bacteriol.* **2005**, *187*, 5090.

(12) (a) Van Ginkel, C. G.; Rikken, G. B.; Kroon, A. G. M.; Kengen, S. W. M. *Arch. Microbiol.* **1996**, *166*, 321. (b) Stenklo, K.; Thorell, H. D.; Bergius, H.; Aasa, R.; Nilsson, T. *J. Biol. Inorg. Chem.* **2001**, *6*, 601. (c) Xu, J.; Logan, B. E. *J. Microbiol. Meth.* **2004**, *271*, 3539. (d) Bender, K. S.; O'Connor, S. A.; Cakraborty, R.; Coates, J. D.; Achenbach, L. A. *Appl. Environ. Microb.* **2002**, *68*, 4820. (e) Streit, B. R.; DuBois, J. L. *Biochemistry* **2008**, *47*, 5271. (f) Lee, A. Q.; Streit, B. R.; Zdilla, M. J.; Abu-Omar, M. M.; DuBois, J. L. *Proc. Natl. Acad. Sci. U.S.A.* **2008**, *105*, 15654–15659.

(13) Hagedoorn, P. L.; Geus, D. C.; Hagen, W. R. *Eur. J. Biochem.* **2002**, *269*, 4905.

(14) Fábián, I. *Coord. Chem. Rev.* **2001**, *216−217*, 449.

(15) Slaughter, L. M.; Collman, J. P.; Eberspacher, T. A.; Brauman, J. I. *Inorg. Chem.* **2004**, *43*, 5198.

(16) Meunier, B.; de Visser, S. P.; Shaik, S. *Chem. Rev.* **2004**, *104*, 3947.

(17) (a) McLain, J. L.; Lee, J.; Groves, J. T. In *Biomimetic Oxidations Catalyzed by Transition Metal Complexes*; Meunier, B., Ed.; Imperial College Press: London, 2000, pp 91−169. (b) Meunier, B.; Bernadou, J. *Top. Catal.* **2002**, *21*, 47. (c) Watanabe, Y. In *The Porphyrin Handbook*; Kadish, K. M., Smith, K. M., Guilard, R., Eds.; Academic Press: New York, 2000, Vol. *4*, pp 97−117.

(18) (a) Song, W. J.; Ryu, Y. O.; Song, R.; Nam, W. *J. Biol. Inorg. Chem.* **2005**, *10*, 294. (b) Koppenol, W. H. *J. Am. Chem. Soc.* **2007**, *129*, 9686. (c) Machii, K.; Watanabe, Y.; Morishima, I. *J. Am. Chem. Soc.* **1995**, *117*, 6691. (d) Vaz, A. D. N.; McGinnity, D. F.; Coon, M. J. *Proc. Natl. Acad. Sci. U.S.A.* **1998**, *95*, 3555. (e) Toy, P. H.; Dhanabalasingam, B.; Newcomb, M.; Hanna, I. H.; Hollenberg, P. F. *J. Org. Chem.* **1997**, *62*, 9114. (f) Nam, W.; Lim, M. H.; Moon, S. K.; Kim, C. *J. Am. Chem. Soc.* **2000**, *122*, 10805. (g) Collman, J. P.; Zeng, L.; Decréau, R. A. *Chem. Commun.* **2003**, 2974. (h) Wang, S. H.; Mandimutsira, B. S.; Todd, R.; Ramdhanie, B.; Fox, J. P.; Goldberg, D. P. *J. Am. Chem. Soc.* **2004**, *126*, 18.

(19) (a) Nam, W.; Choi, S. K.; Lim, M. H.; Rohde, J.-U.; Kim, I.; Kim, J.; Kim, C.; Que, L., Jr *Angew. Chem., Int. Ed.* **2003**, *42*, 109. (b) Collman, J. P.; Chien, A. S.; Eberspacher, T. A.; Brauman, J. I. *J. Am. Chem. Soc.* **2000**, *122*, 11098. (c) Nam, W.; Lim, M. H.; Lee, H. J.; Kim, C. *J. Am. Chem. Soc.* **2000**, *122*, 6641.

(20) Zdilla, M. J.; Lee, A. Q.; Abu-Omar, M. M. *Angew. Chem., Int. Ed.* **2008**, *47*, 7697–7700.

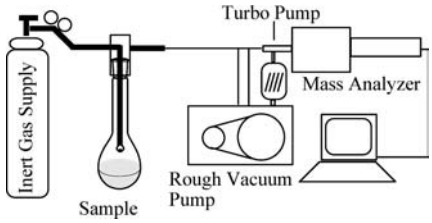

Figure 2. Diagram of the RGA. The sample head space is swept with an inert gas, which is pulled through a 1 m long capillary using a rough vacuum pump. A small portion of the remaining gas is pulled into the high-vacuum region by a turbo pump and analyzed by quadrupole mass spectrometry. The instrument allows the simultaneous monitoring of numerous masses for each experiment.

mass spectrometer (electron impact). The instrument is illustrated in Figure 2. Typical yields of O_2 from dismutation by catalytic amounts of Fe(Por) complexes **1**−**3** are given in Table 1. Other studies have implicated chlorine dioxide (ClO_2) as an important species in chlorite redox chemistry and decomposition.[9] However, we did not observe ClO_2 via RGA or EPR[21] under our conditions. Given the sensitivity of EPR and of our mass spectrometer RGA (10^{-9} Torr), it is compelling to conclude that ClO_2 is not formed/accumulated by our catalytic reactions to any appreciable extent.

Dioxygen formation from ClO_2^- was monitored in phosphate buffer (pH 7.14) prepared using ^{18}O-labeled water as the solvent to test for incorporation of oxygen from water into produced O_2. A small amount of ^{18}O incorporation was seen for Fe(TF_4TMAP) (of the total O_2 formed, 1.4% $^{18}O-^{16}O$, 0.4% $^{18}O-^{18}O$), and no incorporation was observed for Fe(TPPS) or Fe(TMAP). These results are summarized in Table 1.

Isotopically labeled chlorite ions were employed in a double-crossover experiment to probe for scrambling of oxygen atoms in product O_2. An isotopically enriched (77%) sample of chlorite was disproportionated with an equivalent amount of ^{16}O chlorite. The result shows predominantly mass peaks at 32 ($^{16}O_2$) and 36 ($^{18}O_2$) with a smaller peak at 34 ($^{16}O^{18}O$) consistent with the incompletely enriched ^{18}O sample (Table 1, entries 9 and 10).

2,2′-Azino-bis(3-ethylbenzothiazoline-6-sulfonic acid) (ABTS) scavenges $Fe^{IV}(Por)^{\bullet+}$ (Compound I) and $Fe^{IV}(Por)$ (Compound II) species to form $Fe^{III}(Por)$ and the stable $ABTS^{\bullet+}$ cation radical.[22] The effect of ABTS on oxygen formation was tested by including a 1.4-fold excess of ABTS over ClO_2^- during catalysis. Fe(TF_4TMAP) and Fe(TPPS) were tested as catalysts. Presence of ABTS resulted in a modest increase in the yield of O_2 for both catalysts (Table 1, entries 4 and 5).

Hypochlorite was tested as a substrate for oxygen formation. While use of Fe(TF_4TMAP) as a catalyst resulted in quantitative conversion to O_2, neither Fe(TPPS) nor Fe(TMAP) resulted in formation of O_2 from ClO^- (Table 1). Examination of the oxygen product formed in $H_2{}^{18}O$ as solvent demonstrated a significant incorporation of ^{18}O into the O_2 product (Table 1, entry 12).

Analysis of Solution Species by Ion Chromatography (IC). Ion chromatography was used to identify and quantify anionic products resulting from iron-porphyrin-catalyzed decomposition of chlorite and hypochlorite. IC indicates the complete consumption of reactant ClO_2^- to give Cl^- and ClO_3^- as the major ionic products in an approximate 1:2 ratio for Fe(TPPS) and Fe(TMAP). The ratio of ClO_3^-: Cl^- is about 1:1.5 for Fe(TF_4TMAP). When chlorite decomposition was carried out in the presence of a 10-fold excess of ABTS, ClO_3^- formation was suppressed, and the sole observed anionic product was Cl^-. In the case of hypochlorite disproportionation catalyzed by Fe(TF_4TMAP), Cl^- is the sole anionic product of the reaction. Exact yields of ions are summarized in Table 1. Ion chromatograms are available in the Supporting Information.

Mass Spectrometry Analysis of Chlorate Product. To obtain mechanistic information on the source of oxygen in the chlorate product, we employed isotopically labeled $H_2{}^{18}O$ as solvent in Fe(Por) catalyzed decomposition of chlorite. Product solutions were analyzed by ESI mass spectrometry to determine the degree of ^{18}O incorporation into ClO_3^-. Using Fe(TPPS) as a catalyst, 57% ^{18}O incorporation was observed in the chlorate product as $Cl^{16}O_2{}^{18}O^-$, entry 7, Table 1, (spectrum available in the Supporting Information). Therefore, only a single ^{18}O was incorporated. Multiple incorporation products ($Cl^{16}O^{18}O_2^-$, $Cl^{18}O_3^-$) were not detected. In the case of Fe(TF_4TMAP) as a catalyst, no ^{18}O incorporation (from $H_2{}^{18}O$ solvent) was observed (Table 1, entry 6).

Absorption Spectroscopy and Kinetics. Disappearance of ClO_2^- was monitored by following its absorption band at 260 nm. Kinetic experiments were designed to keep the catalyst concentration at a minimum such that the UV charge transfer (CT) bands due to the Fe(Por) are of much lower intensity than that of chlorite. This condition is not suitable for Fe(TPPS) and Fe(TMAP), as these catalysts are easily bleached by large excesses of chlorite. Fe(TF_4TMAP), however, is quite resistant to bleaching and hence suitable for kinetics analysis.

When a solution of chlorite (2.4−24 mM) was monitored in the presence of 0.05 mol % Fe(TF_4TMAP), an induction period was seen before the approximate first-order disappearance of the chlorite band at 260 nm (Figure 3). The induction period is approximately 0.5−1.0 s depending upon initial concentration of ClO_2^- (Figure 3). Similar behavior was also seen for Fe(TPPS) as a catalyst; however, complete ClO_2^- consumption was not achieved under these conditions because of bleaching of the catalyst (vide supra). On the basis of rapid repeat scans by stopped-flow spectroscopy on the Fe(TF_4TMAP) catalyst, this induction period corresponds to the formation of Compound II (Figure 4), which remains as a steady state intermediate throughout the reaction and accounts for the bulk of the catalyst. This identification was made based on comparison of the spectrum with known

(21) Quiroga, S. L.; Churio, M. S.; Perissinotti, J. L. *Appl. Magn. Reson.* **2002**, *22*, 115.
(22) (a) Zipplies, M. F.; Lee, W. A.; Bruice, T. C. *J. Am. Chem. Soc.* **1986**, *108*, 4433. (b) Huenig, S.; Balli, H.; Conrad, H.; Schott, A. *Justus Liebigs Ann. Chem.* **1964**, *676*, 32,36, 52.

Table 1. Results of Catalytic Decomposition of ClO_2^- and ClO^- by Fe(Por) Model Complexes[a]

entry	substrate	catalyst	special conditions	products (% yield or % enrichment)
1	ClO_2^-	Fe(TF_4TMAP)		O_2 (18), Cl^- (36),ClO_3^- (56)
2	ClO_2^-	Fe(TPPS)		O_2 (3), Cl^- (31),ClO_3^- (63)
3	ClO_2^-	Fe(TMAP)		O_2 (7), Cl^- (32),ClO_3^- (62)
4	ClO_2^-	Fe(TF_4TMAP)	ABTS[b,e]	O_2 (30), Cl^-
5	ClO_2^-	Fe(TPPS)	ABTS[b,e]	O_2 (5), Cl^-
6	ClO_2^-	Fe(TF_4TMAP)	$H_2{}^{18}O$	$^{16}O_2$ (98.2), $^{16}O^{18}O$ (1.4),$^{18}O_2$ (0.4), $Cl^{16}O_3^-$ (100)[c]
7	ClO_2^-	Fe(TPPS)	$H_2{}^{18}O$	$^{16}O_2$ (100), $Cl^{16}O_3^-$ (43), $Cl^{16}O_2{}^{18}O^-$ (57)[c]
8	ClO_2^-	Fe(TF_4TMAP)	$KHSO_5$[d]	O_2 (15), Cl^- (35),ClO_3^- (57)
9	$Cl^{18}O_2^-$	Fe(TF_4TMAP)	$H_2{}^{16}O$	$^{16}O_2$ (6%), $^{16}O^{18}O$ (34%), $^{18}O_2$ (60%)[c]
10	$Cl^{18}O_2^-$ and $Cl^{16}O_2^-$, 1:1	Fe(TF_4TMAP)	$H_2{}^{16}O$	$^{16}O_2$ (54%), $^{16}O^{18}O$ (17%), $^{18}O_2$ (29%)[c]
11	ClO^-	Fe(TF_4TMAP)[e]		O_2 (100), Cl^-
12	ClO^-	Fe(TF_4TMAP)	$H_2{}^{18}O$	$^{16}O_2$ (22), $^{16}O^{18}O$ (45), $^{18}O_2$ (33)[c]

[a] All yields are calculated based on chlorite. Yields of oxygen were determined from integration of the RGA trace at $m/z = 32$ calibrated with O_2 standards. Yields of ions were determined using ion chromatography by integration of ion signals, and by comparison to a standard curve. [b] O_2 evolution was measured with an excess of ABTS over chlorite. [c] % in these entries refers to % of total product content. The value represents the level of incorporation of ^{18}O into the product, not the % yield. The reactions were analyzed by mass spectrometry, electron-impact for gases (RGA), and ESI for the chlorate ion. [d] HSO_5^- was added to the catalyst to convert it to Compound II before the addition of ClO_2^-. [e] Ions were identified but not quantified. However, Cl^- was the only chlorine containing species by IC.

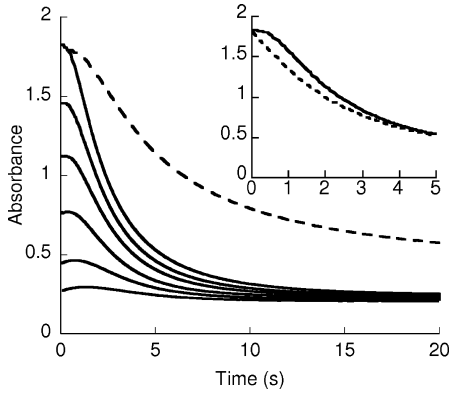

Figure 3. Absorption of chlorite at 260 nm after addition of Fe(TF_4TMAP) catalyst. Solid lines: [Fe(TF_4TMAP)] = 6.2×10^{-6}; $[ClO_2^-]_0 = 0.012$, 0.0096, 0.0072, 0.0048, 0.0024, and 0.0012 M. Dotted line: [Fe(TF_4TMAP)] = 3.1×10^{-6} M; $[ClO_2^-]_0 = 0.012$ M. Inset: [Fe(TF_4TMAP)] = 6.2×10^{-6}; $[ClO_2^-]_0 = 0.012$; chlorite solution added to Fe^{III} form of the catalyst (solid line), and chlorite solution added to Compound II form of the catalyst (dashed line), which was prepared in situ by the addition of HSO_5^- to Fe(TF_4TMAP).

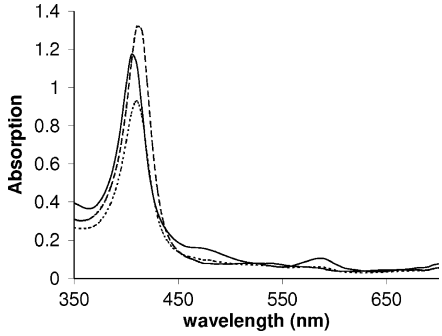

Figure 4. Absorption spectra showing Fe^{III}(TF_4TMAP) (solid line), O=Fe^{IV}(TF_4TMAP) 1 s after addition of ClO_2^- (dashed line), and the return of catalyst to the Fe^{III} form about 30 min after reaction with some bleaching (dotted line).

forms of Compound II of analogous porphyrins.[23] At low concentrations of chlorite, a slight rise in absorbance is seen because of absorbance of compound II at 260 nm. At higher concentrations of chlorite, this absorbance change is too small to observe and an induction period instead is seen.

Kinetic traces fit well to a single exponential equation (i.e., first order in chlorite, the limiting reagent) after the induction period. The curvature of the plot of k_ψ versus catalyst (Figure 5A) demonstrates that the order in Fe(TF_4TMAP) is complex. Additionally, a plot of k_ψ versus initial chlorite concentration (Figure 5B) demonstrates that, while the chlorite disappearance fits well to a single exponential, the order in chlorite is actually larger than first order (positive slope) rather than the expected horizontal line if indeed chlorite dependence is strictly first order. To get a more detailed look at chlorite dependence, an instantaneous rates method was used in the analysis of the chlorite dependent data (Figure 5C).[24] Concentration dependences (Figure 5, panels A,C) fit best to a mixed 1st−2nd order rate equation.[25]

Generation of Compound II before Addition of ClO_2^-. To test if Compound II is the active form of the catalyst for O_2 formation from ClO_2^-, we generated (TF_4TMAP)Fe^{IV}(O) in situ by the addition of $KHSO_5$ to Fe^{III}(TF_4TMAP). HSO_5^- and other oxidants are known to result in compound I ((por$^{\bullet+}$)Fe^{IV}(O)), which quickly conproportionates with $[Fe^{III}(Por)(H_2O)]^+$ to generate 2 equiv of compound II (eq 2).[23]

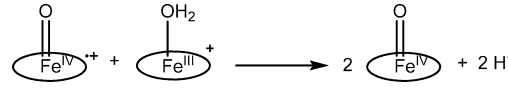

(2)

Decomposition of chlorite was carried out as described above with Compound II as the starting form of the catalyst. It should be noted that while a 3-fold excess of $KHSO_5$ over

(23) Bell, S. E.; Cooke, P. R.; Inchley, P.; Leanord, D. R.; Smith, J. R. L.; Robbins, A. *J. Chem. Soc., Perkin Trans. 2* **1991**, 549.

(24) Reaction rates were determined by fitting a line through the inflection point (determined by 2nd derivative method) of the kinetic traces in Figure 3, the slope of which corresponds to the instantaneous rate under steady-state conditions. The rate is normalized to catalyst by dividing the instantaneous rate by $[Fe(TF_4TMAP)]_T$. In Fig. 5C, concentration of ClO_2^- was determined using the molar absorptivity (ε) at 260 nm based on the absorbance value at the inflection point in each plot. Total concentration of the catalyst Fe(TF_4TMAP) was assumed constant for each plot under steady-state conditions, i.e., catalyst degradation was negligible over the course of reaction.

(25) A detailed derivation of the rate law is given in the Supporting Information. While our 1st order approximation used in the treatment of kinetic data is not strictly mathematically correct (since dependences are really mixed-order), the treatment is sufficient to invalidate the possibility that the dependences are 1st order and to demonstrate the existence of a more complex kinetic profile.

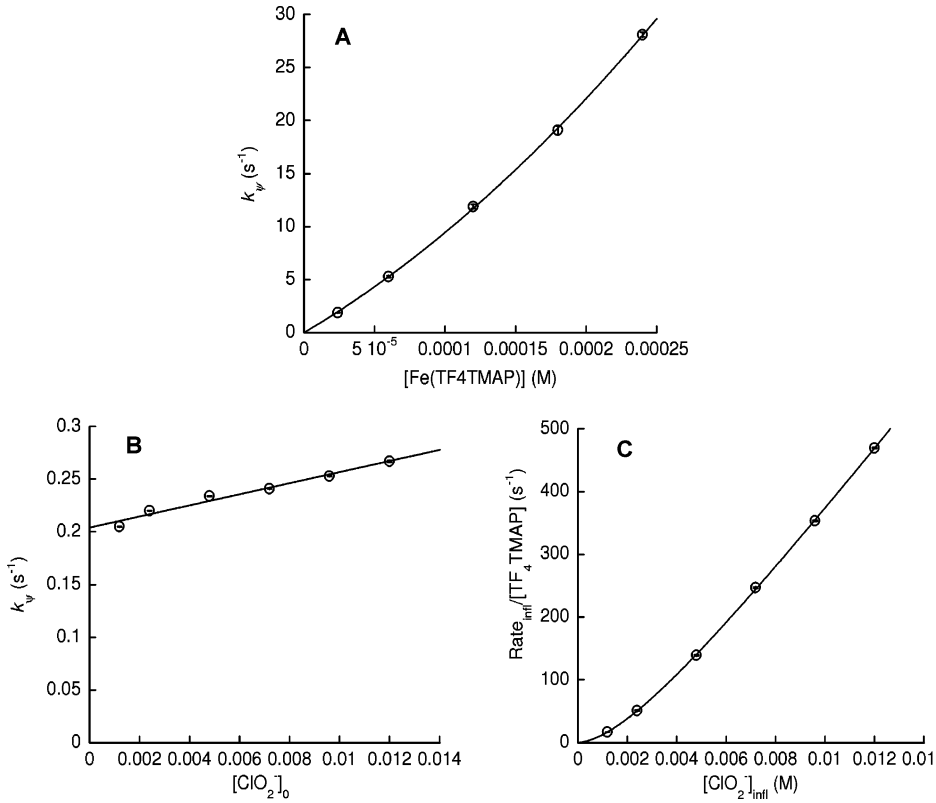

Figure 5. Kinetics of chlorite consumption. Fits for A and C are to mixed 1st−2nd order rate equation of the general form: $d[A]/dt = (a[A]^2 + b[A])/(c + [A])$.[25] Fit for B is to a line. (A) Dependence of k_ψ on catalyst concentration. Values of k_ψ determined from exponential fits of kinetic traces. $[ClO_2^-]_0 = 0.038$ M; $R = 0.999$. (B) Dependence of k_ψ on initial chlorite concentration. Values of k_ψ determined from exponential fits of kinetic traces. $R = 0.987$. (C). Chlorite dependence determined by computing $Rate_{infl}/[Fe(TF_4TMAP)]_0$, where $Rate_{infl}$ and $[ClO_2^-]_{infl}$ refer to the reaction rate and chlorite concentration at the curve's inflection point, $[Fe(TF_4TMAP)]_0 = 6.2 \times 10^{-6}$ M; $R = 0.999$.

Fe was used to ensure that the majority of the catalyst is in the form of Compound II, the ClO_2^- added subsequently is in a 740-fold excess over HSO_5^-. Thus, the majority of oxidant in the system is ClO_2^- and not HSO_5^-.

When ClO_2^- is added to $Fe^{IV}(O)(TF_4TMAP)$ (Compound II) the distribution of products by IC is very similar to that starting with $Fe^{III}(TF_4TMAP)$ form of the catalyst (Table 1), suggesting the general reaction profile is not affected. However, monitoring the disappearance of ClO_2^- at 260 nm by stopped-flow shows the disappearance of the induction period (Figure 3, inset). More importantly, O_2 formation is inhibited when Compound II form of the catalyst is used. Figure 6 shows comparative traces for the evolution of O_2 measured by RGA. It can be seen from Figure 6 that the yield of O_2 is decreased when $(TF_4TMAP)Fe^{IV}(O)$ is the starting catalyst versus $Fe^{III}(TF_4TMAP)$.

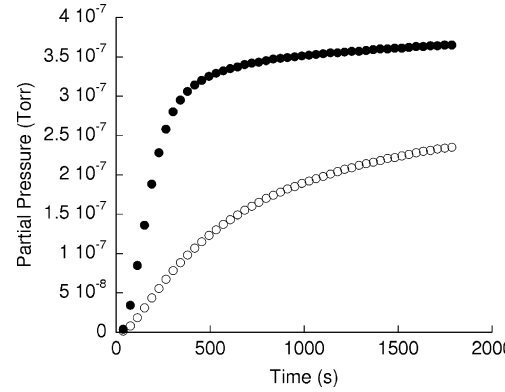

Figure 6. Plots of total O_2 production from chlorite decomposition. $[Fe(TF_4TMAP)] = 2.4$ mM; $[ClO_2]_0 = 91$ mM. Reaction started with Fe^{III} form of the catalyst (●) and after addition of 7.1 mM HSO_5^- to convert catalyst to Compound II, $O{=}Fe^{IV}(TF_4TMAP)$ (○).

Discussion

The simplest stoichiometry one can envision for chlorite dismutation is that described in eq 1. One chlorite ion dismutes to one chloride ion and one molecule of dioxygen: $ClO_2^- \rightarrow Cl^- + O_2$. In our model systems, O_2 formation constitutes only one of the products based on the complete consumption of chlorite; see yield of O_2 in Table 1, 18% in the case of $Fe(TF_4TMAP)$, and less than 10% in the case of the other two catalysts. In the latter two cases, catalysts **2** and **3**, chlorite is largely decomposed via a pathway that does not afford dioxygen. For this reason, it is not straightforward to address the issue of reaction stoichiometry for the formation of O_2. An easier issue to address first is the bulk reaction, which according to the product distribution for catalysts **2** and **3** (2:1 ClO_3^-/Cl^-) is as follows:

$$3ClO_2^- \xrightarrow{\text{cat. 2 or 3}} Cl^- + 2ClO_3^- \qquad (3)$$

Reaction 3 is the dominant one for Fe(TPPS) and Fe(TMAP), which give low yields of O_2. On the other hand, while reaction 3 does occur for $Fe(TF_4TMAP)$, it is not the only significant pathway (vide infra).

Scheme 1. Reaction Mechanism for ClO_2^- Dismutation to Cl^- and ClO_3^-

$$ClO_2^- + Fe^{III}(Por) \xrightarrow{k_{III}} O{=}Fe^{IV}(Por)^{\cdot+} + ClO^-$$
$$O{=}Fe^{IV}(Por)^{\cdot+} + Fe^{III}(Por)(H_2O) \xrightarrow{k_{con}} 2\ O{=}Fe^{IV}(Por) + 2\ H^+ \quad \text{Initiation}$$

$$O{=}Fe^{IV}(Por) + ClO_2^- \xrightarrow{k_{IV}} Fe^{II}(Por) + ClO_3^- \text{ (slow)}$$
$$ClO_2^- + Fe^{II}(Por) \xrightarrow{k_{II}} O{=}Fe^{IV}(Por) + ClO^- \quad \text{Catalysis}$$
$$ClO^- + Fe^{II}(Por) \xrightarrow{k_f} O{=}Fe^{IV}(Por) + Cl^-$$
$$O{=}Fe^{IV}(Por) + ClO_2^- \xrightarrow{k_{IV}} Fe^{II}(Por) + ClO_3^- \text{ (slow)}$$

$$3\ ClO_2^- \longrightarrow Cl^- + 2\ ClO_3^- \quad \text{Overall}$$

The presence of an induction period in the kinetic profiles for chlorite consumption indicates that the active form of the catalyst is not present at the onset of reaction. Rapid scan absorption spectroscopy implicates the iron(IV) oxo compound II ($O{=}Fe^{IV}(Por)$) as the active catalyst since the appearance of this spectrum coincides with the induction period. Compound II is known to form in water-soluble porphyrin systems from the conproportionation of Compound I and $Fe^{III}(Por)(OH_2)$, eq 2.[23]

The activity of $(Por)Fe^{IV}(O)$ as the catalyst for chlorite consumption was confirmed by generating Compound II initially using HSO_5^- as an oxidant, and then adding chlorite. This test resulted in disappearance of the induction period. We therefore propose reaction Scheme 1 for reaction 3 catalyzed by Fe^{II}/Fe^{IV} redox couple.

The last two steps of catalysis represent the catalytic formation of chlorate from chlorite and hypochlorite. While this reaction is spontaneous without a catalyst,[26] it is slow under our conditions, and would result in accumulation of hypochlorite without the invocation of the catalyst. Such accumulation of OCl^- would result in O_2 formation in the presence of $Fe(TF_4TMAP)$. This mechanism for O_2 formation will be considered shortly.

We tested the validity of the mechanism in Scheme 1 using ABTS, 2,2′-Azino-bis(3-ethylbenzothiazoline-6-sulfonicacid), as a scavenger for $Fe^{IV}{=}O$ species. ABTS reduces Compounds I and II in a fast reaction, which should, in theory, destroy catalytically active Compound II species, and return the oxidation state to Fe(III). Additionally, ABTS is reactive toward ClO^- in the presence of other ions[27] and could potentially remove these species from the catalytic cycle as well. When the reaction is carried out in the presence of excess ABTS, the sole anionic product is indeed Cl^- according to IC with no formation of ClO_3^-. This result suggests that ABTS successfully scavenges Compound II since it is this species that gives rise to chlorate. Chloride is produced from the reduction of ClO^- by k_f in Scheme 1 and possibly by reaction of ClO^- with ABTS.

$H_2{}^{18}O$ is commonly used to test the involvement of accumulated $Fe{=}O$ species in cytochrome P450 model reactions because it exchanges with $Fe{=}O$ via a tautomeric mechanism (Scheme 2).[28] Accumulated $Fe{=}O$ species are

Scheme 2. Oxygen Exchange with Solvent in Porphyrin $Fe{=}O$ Complexes

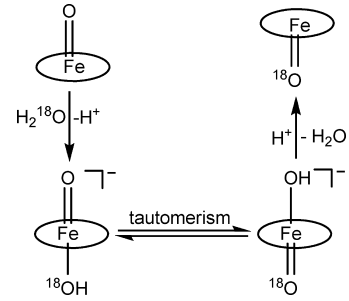

therefore expected to undergo ^{18}O exchange and incorporate the labeled isotope into the products.

Table 1 shows that $Fe(TF_4TMAP)$ does not facilitate ^{18}O incorporation into chlorate, but this is attributed to the fact that the TF_4TMAP porphyrin is known to undergo tautomeric exchange much more slowly than other water-soluble porphyrins.[29] The Fe(TPPS) catalyst, however, shows significant (57%) incorporation of a single ^{18}O into the chlorate product ($Cl^{16}O_2{}^{18}O^-$) as determined by negative mode ESI mass spectrometry (see Supporting Information). No evidence of double ($Cl^{16}O^{18}O_2^-$) or full ($Cl^{18}O_3^-$) incorporation is seen, suggesting that there is a direct transfer of ^{18}O to chlorite ion without scrambling of the oxygen atoms on chlorine. Additionally, control experiments demonstrate that ClO_3^- and ClO_2^- do not exchange their oxygen atoms with $H_2{}^{18}O$ fast enough at neutral pH to explain ^{18}O incorporation without invoking participation of the iron porphyrin.

While the ^{18}O incorporation is seen in chlorate, the dioxygen product does not show ^{18}O incorporation, which suggests that Compound II, which exchanges its oxo with bulk water, is not responsible for the O_2 production pathway. Further evidence that Compound II is not the active catalyst for O_2 production comes from the data in Figure 6, which demonstrates that starting with Compound II, $O{=}Fe^{IV}(Por)$, as the catalyst results in less dioxygen formation. Some oxygen is still produced in this reaction because Compound II can revert to Fe(III) as demonstrated by the spectra in Figure 4. This most likely occurs via conproportionation of $(Por)Fe^{IV}(O)$ with $Fe^{II}(Por)$.

$$[O{=}Fe^{IV}(Por)] + [Fe^{II}(Por)] + 2H^+ \rightarrow 2[Fe^{III}(Por)]^+ + H_2O \quad (4)$$

Lastly, addition of ABTS to the reaction catalyzed by $Fe^{III}(TF_4TMAP)$, **3**, increases O_2 yield (entry 4 vs 1 in Table 1). This result provides additional support to the notion that Fe^{III}, not $O{=}Fe^{IV}(Por)$, is responsible for O_2 formation. ABTS acts to destroy Compound II and regenerate the Fe^{III} form of the catalyst, which encourages dioxygen formation.

Hence, possible mechanisms for dioxygen formation are outlined in Scheme 3. In pathway A, accumulated hypochlorite from chlorite decomposition is catalytically decomposed to O_2 via an oxoferryl intermediate. In this mechanism, hypochlorite acts as a nucleophile toward the oxo ligand, resulting in a proposed short-lived peroxyhypochlorite ad-

(26) (a) Lister, M. W *Can. J. Chem.* **1956**, *34*, 465. (b) Gordon, G.; Tachiyashiki, S. *Environ. Sci. Technol.* **1991**, *25*, 468.
(27) Pinkernell, U.; Nowack, B.; Gallard, H.; Von Gunten, U. *Wat. Res.* **2000**, *34*, 4343.
(28) Primus, J.-L.; Teunis, K.; Mandon, D.; Veeger, C.; Rietjens, I. M. C. M. *Biochem. Biophys. Res. Commun.* **2000**, *272*, 551.
(29) La, T.; Miskelly, G. M. *J. Am. Chem. Soc.* **1995**, *117*, 3613.

Scheme 3. Possible Mechanisms for Dioxygen Formation from Chlorite

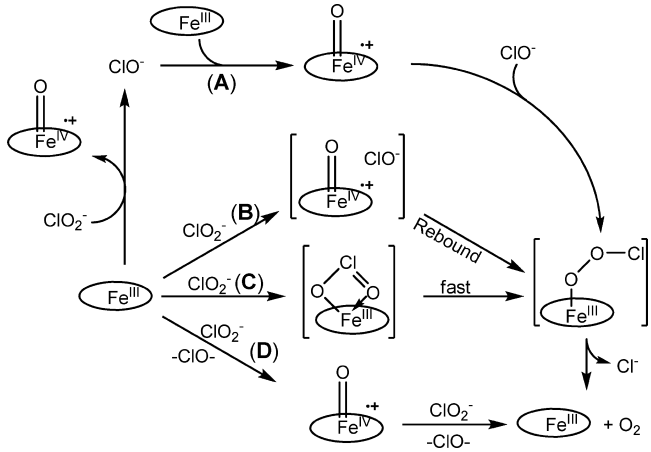

duct, which rapidly decomposes to O_2 and Cl^-. This mechanism is proposed based on the observation that Fe(TF$_4$TMAP) quantitatively forms dioxygen and Cl^- from ClO^- (entry 11, Table 1). In mechanism B, chlorite transfers an oxygen atom to iron, and then rebounds in a subsequent fast step to give O_2 and chloride. The quantitative formation of dioxygen from hypochlorite suggests that this mechanism is feasible as long as hypochlorite rebounds with Compound I faster than diffusing into solution. Similar to mechanism A, the nucleophilic attack of ClO^- on the oxoferryl is proposed to give the intermediate peroxyhypochlorite adduct. Mechanism C is formation of O_2 from rearrangement of a chlorite adduct. This mechanism is kinetically indistinguishable from mechanism B and would likely result in the same Fe$-$O$_2$Cl moiety as A and B. Finally mechanism D is similar to mechanism B except ClO^-, formed from reaction of chlorite with Fe^{III}, escapes into solution, and Compound I requires a second chlorite molecule to give dioxygen.

Pathway A can be excluded based on isotope labeling experiments for hypochlorite dismutation. OCl^- dismutation in $H_2{}^{18}O$ results in substantial ^{18}O incorporation into the O_2 product (entry 12, Table 1). This occurs because of the rapid exchange of oxygen atoms between water and the hypochlorite ion[30] prior to reaction with the catalyst. This result is in contrast to chlorite dismutation carried out in $H_2{}^{18}O$, which shows no ^{18}O incorporation into product oxygen (entries 6 and 7, Table 1). If O_2 formation from chlorite was occurring because of accumulated ClO^- as in pathway A, ^{18}O incorporation would have been observed into the O_2 product.

The remaining mechanisms cannot be distinguished by kinetic analysis. Speciation of the catalyst into Compound II complicates the theoretical rate equations (see Supporting Information for rate law derivation) and any of the mechanisms B, C, and D satisfy the complex kinetic profiles (Figure 5). It should be noted that while condensation of Fe^{III}(Por) complexes to form dinuclear μ-oxo complexes is known,[31] and could further complicate kinetics analysis, the Fe(TF$_4$TMAP) porphyrin used for kinetic studies herein is resistant to dinuclear complex formation.[32a]

Nevertheless, mechanism D can be rejected on the basis of an ^{18}O-labeling crossover experiment using a 1:1 mixture of ClO_2^- and isotopically labeled $Cl^{18}O_2^-$. The crossover experiment gave a majority of $^{16}O_2$ and $^{18}O_2$ based on mass spectrometry. The intensity of the smaller $^{16}O^{18}O$ mass peak is consistent with the incomplete enrichment of the $Cl^{18}O_2^-$ starting sample. This result is contrary to the expectation of mechanism D, which would result in a 1:2:1 binomial distribution of $^{16}O_2$, $^{16}O^{18}O$, and $^{18}O_2$, respectively. Therefore, this double-crossover result confirms that formation of O_2 from chlorite is concerted, each oxygen in the O_2 product originates from the same chlorite ion. While mechanisms B and D both involve the same intermediate at iron (Compound I), the intermediate in mechanism B is an ion pair that undergoes rebound faster than competing bimolecular reactions. Rebound reactions in iron dependent oxygenases have been shown to have rate constants $\geq 10^8$ s^{-1}.[17a,33]

Discrimination between mechanisms B and C by experimental means is daunting because of their indistinguishable kinetic form, identical expectations for ^{18}O-labeling experiments, and the fact that the intermediate state of either mechanism would be short-lived. This admitted, one could argue that the observation of Compound II (Figure 4) demonstrates the feasibility of formation of oxoferryl from Fe^{III}(Por) and ClO_2^- via mechanism B. Deactivation of the O_2-evolving catalyst would thereby occur via escape of hypochlorite from the ion-pair to give Compound I, which relaxes to Compound II (via conproportionation with Fe^{III}). Conversely, while some coordination complexes of chlorite are known,[14] there is no chemical precedent for metal-bound chlorite rearrangement on a metal ion without changes in the chlorine oxidation state, as in mechanism C. Given the observation of ferryl species in the system, and the lack of precedent for molecular rearrangement of chlorite bound to a metal, mechanism C is disfavored, though not rigorously discarded.

The energetics of chlorite ion degradation to either dioxygen and chloride or chlorate and chloride are favorable: $ClO_2^- \rightarrow Cl^- + O_2$ ($\Delta G° = -149$ kJ mol^{-1}); $3ClO_2^- \rightarrow Cl^- + 2ClO_3^-$ ($\Delta G° = -189$ kJ mol^{-1}).[34] It is interesting to note that the enzyme chlorite dismutase has evolved an exquisite selectivity for the thermodynamically less favorable dioxygen evolving pathway. On the other hand, degradation of the chlorite ion to chlorate and chloride is overwhelmingly dominant for the model complexes investigated herein especially catalysts **2** and **3**; only in the case of the fluorinated porphyrin, catalyst **1**, does the oxygen evolving pathway

(30) Robert, A.; Meunier, B. C. R. *Acad. Sci. II C* **2000**, *3*, 771.

(31) (a) Harris, F. L.; Toppen, D. L. *Inorg. Chem.* **1978**, *17*, 71. (b) Kobayashi, N.; Koshiyama, M.; Osa, T.; Kuwana, T. *Inorg. Chem.* **1983**, *22*, 3608. (c) Trondeau, G. A.; Wilkings, R. G. *Inorg. Chem.* **1986**, *25*, 2745. (d) Miskelly, G. M.; Webley, W. S.; Clark, C. R.; Buckingham, D. A. *Inorg. Chem.* **1988**, *27*, 3773. (e) Bell, S. E. J.; Hill, J. N.; Hester, R. E.; Shwcross, D. R.; Lindsay Smith, J. R. *J. Chem. Soc., Faraday Trans.* **1990**, 4017.

(32) (a) La, T.; Richards, R.; Miskelly, G. M. *Inorg. Chem.* **1994**, *33*, 3159. (b) Kadish, K. M.; Araullo-McAdams, C.; Han, B. C.; Franzen, M. M. *J. Am. Chem. Soc.* **1990**, *112*, 8364.

(33) (a) He, X.; Ortiz de Montellano, P. R. *J. Biol. Chem.* **2004**, *279*, 39479. (b) Jin, Y.; Libscomb, J. D. *Biochim. Biophys. Acta* **2000**, *1543*, 47.

(34) Shriver, D. F.; Atkins, P. *Inorganic Chemistry*, 3rd ed.; W.H. Freeman and Co.: New York, 2003; p 700.

Scheme 4

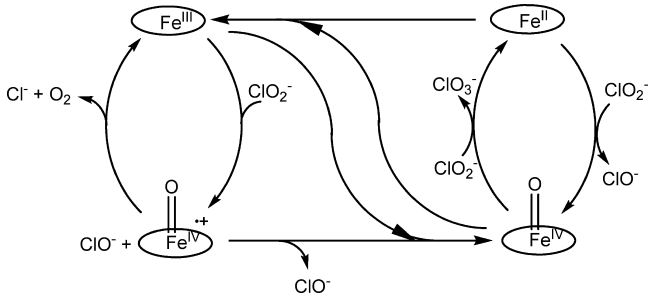

become somewhat competitive accounting for 1/5 of the product distribution.[35]

Conclusion

We have reported herein the first functional model system for the enzyme chlorite dismutase. The mechanistic results are summarized in Scheme 4. The initial step of the reaction is the formation of Compound I and hypochlorite via oxygen atom transfer. Rebound of the intermediate hypochlorite with Compound I results in O_2 and Cl^- formation in a biomimetic model reaction for chlorite dismutase. The catalyst deactivates when hypochlorite diffuses into solution before rebound, resulting in conproportionation of the resulting Compound I with an equivalent of Fe^{III}(Por) to form Compound II, at which point the catalyst enters a new cycle for which the Fe^{II}/Fe^{IV}(O) cycle disproportionates chlorite into Cl^- and ClO_3^- in 1:2 molar ratio. This form of the catalyst can be "rescued" back to the oxygen formation cycle by the one electron reductant ABTS, which converts Compound II to Fe^{III}. In comparison, the biological enzyme chlorite dismutase catalyzes the decomposition of chlorite exclusively to chloride and dioxygen without formation of chlorate. A recent mechanistic probe of the enzyme concluded that the enzyme must impede hypochlorite diffusion from the active pocket to solution by forcing its rebound with transient Compound I.[12f] While the described model system exhibits a biomimetic rebound reaction, the absence of protein permits the ClO^- anion to diffuse into solution resulting in catalyst deactivation and ClO_3^- formation. In an effort to develop environmentally useful bioinspired catalysts, future models will employ ligand functionalities designed to retain ClO^- at the catalytic site.

Experimental Section

General Procedures. All reactions were carried out in deionized water obtained from a Millipore Milli-Q Academic TC water purification system. Reagents were used as obtained from Fisher, Baker, Acros, Sigma-Aldrich, GFS, Mid-Centruy, Frontier, and Strem. Sodium chlorite was obtained from GFS chemical as a 98% pure solid. Ion chromatographic analysis suggests that this material is ~95% pure, with a 2.5% chlorate, and a 2.5% unidentified anion(s) impurity. Phosphate buffers were prepared by dissolving of mono- and dibasic sodium phosphate. Ammonium acetate buffers were prepared by dissolution of ammonium acetate and titration to pH 7 with aqueous sodium hydroxide. UV−vis spectra were recorded on a Shimadzu UV-2501PC scanning spectrophotometer. Absorption kinetics experiments were performed using an Applied Photophysics SX.18MV Stopped-Flow Analyzer. Gas evolution was analyzed using an in-house built RGA Mass Spectrometer. Typically, the reaction solution (1−2 mL) was stirred in a custom-made glass RGA cell with a minimum (1−2 mL) head space. An inert carrier gas (Ar or N_2) was drawn over the reaction head space at 2 mL/min by a Varian model SH 100 vacuum pump and analyzed by a Stanford Research Systems RGA 100 mass spectrometer equipped with an Alcatel ATH31 Series turbopump. ESI mass spectra were obtained using a FinniganMAT LCQ mass spectrometer system or a Finnigan LTQ Linear Ion Trap Mass spectrometer in negative ion mode. Sample was introduced by direct infusion from a syringe pump. Ion chromatography was performed on a Dionex DX-500 Liquid Chromatography System equipped with a Dionex LC25 Chromatography Oven, a Dionex ED40 Electrochemical Detector, and a Dionex Ion-Pac AS9-HC ion exchange column. Nine millimolar Na_2CO_3 was used as eluant. Chromatography calibration standards were prepared in the 0.5−60 mM concentration range. Peaks were identified by comparison to standard samples and quantified by comparison of the integrals of the signals to standard curves for the corresponding ion.

[Fe(TF_4TMAP)][OTf^-]$_5$ was prepared from 5,10,15,20-tetrakis(pentafluorophenyl)porphine (Frontier) according to the procedure of Miskelly et al.[32a]

Na_3[Fe(TPPS)] was used as received from Mid-Century chemical company or prepared from (TPPS)H_2 (Strem) according to the procedure of Fleischer et al.[36]

[Fe(TMAP)]Cl_5 was used as obtained from Mid-Century chemical company.

RGA Calibration. Yields of oxygen were determined by integration of the RGA signal and comparison to a calibration curve prepared by the injection of known volumes of oxygen gas. The calibration plots were obtained in the following way: For a 4 mL RGA glass cell, 2 mL of water was added into the cell and stirred to simulate a typical reaction. 50, 125, 250, 375, and 500 μL of air were injected into the RGA cell through a rubber septum. Partial pressure (Torr) of oxygen was monitored against time (seconds) for each calibration point. Integration of the partial pressure versus time graph is plotted against moles of oxygen injected (assuming 20.95% of air is oxygen).

Yield of Oxygen Evolution from ClO_2^- Catalyzed by Fe(TF_4TMAP). [$NaClO_2$] = 91 mM and catalyst concentration of 2.4 mM were used. Partial pressure of O_2 at $m/z = 32$ was recorded with respect to time via RGA using Ar as a carrier gas. For reaction starting with compound II, (TF_4TMAP)Fe^{IV}(O) was generated by adding HSO_5^- to Fe(TF_4TMAP) in the RGA cell before injecting a small volume of $NaClO_2$. Final concentrations of each reagent were as follows: 7.1 mM KHSO5, 2.4 mM Fe(TF_4TMAP), and 91 mM $NaClO_2$. O_2 was quantified by integration of the RGA signal and comparison to standard calibration plots (vide supra).

Oxygen Formation in the Presence of ABTS. Fe(TPPS): Oxygen evolution was monitored in the RGA for reaction of 50 mM $NaClO_2$, 70 mM ABTS, and 2.2 mM catalyst in 0.1 M sodium phosphate buffer, pH 7.1. Fe(TF_4TMAP): Oxygen evolution was monitored by RGA for reaction of 50 mM $NaClO_2$, 70 mM ABTS, and 2.2 mM catalyst in 0.1 M sodium phosphate buffer, pH 7.1.

Test for ^{18}O Incorporation into Oxygen Product. Chlorite dismutation was carried out in oxygen-18 enriched water (95%). Oxygen evolved from the reaction was analyzed using the RGA

(35) Comparison of the thermodynamics of oxo transfer for the employed catalysts and/or the enzyme is not possible because the potentials for Compounds I and II are not available.

(36) Fleischer, E. B.; Palmer, J. M.; Srivastava, T. S.; Chatterjee, A. *J. Am.Chem. Soc.* **1971**, *93*, 3162.

set up as described above, except the carrier gas used was N_2 instead of Ar because of the interfering argon isotope ^{36}Ar. Fe(TPPS): 0.9 M $NaClO_2$, 4.6 mM catalyst, and 1 M sodium phosphate buffer, pH 7.1 were all prepared in oxygen-18 enriched water (95%). 0.1 M $NaClO_2$, 2.6 mM Fe(TF_4TMAP) or Fe(TMAP) and 0.1 M sodium phosphate buffer, pH 7.1 were all prepared in oxygen-18 enriched water (95%).

For hypochlorite dismutation, Fe(TF_4TMAP) (2.8 mM, 2 mL) was prepared in 100 mM phosphate buffer (pH = 7.1) in $H_2{}^{18}O$. A concentrated solution of hypochlorite (1.55 M) was prepared in normal $H_2{}^{16}O$ to prevent exchange of the hypochlorite oxygens with ^{18}O prior to mixing. To initiate reaction, 30 μL hypochlorite solution was added to the solution of catalyst in 2 mL $H_2{}^{18}O$ phosphate buffer.

Test for ^{18}O Incorporation into Chlorate Product. Solutions were prepared in 50 mM ammonium acetate buffer, pH 7.1 in $H_2{}^{18}O$. A 0.25 mL volume of a 2.5 mM Fe(Por) solution was added to 0.25 mL of $NaClO_2$ (40 mM). These solutions were stirred about 20 h and analyzed by ESI mass spectrometry. Control experiments with $NaClO_3$ were performed as well. A 0.25 mL volume of a 2.5 mM Fe(Por) solution was added to 0.25 mL of $NaClO_3$ (40 mM) and stirred 20 h before analysis by ESI mass spectrometry.

Kinetic Measurements on Chlorite Consumption. Kinetic measurements were carried out using a stop flow analyzer by monitoring the absorbance of chlorite at 260 nm ($\varepsilon_{260} = 154\ M^{-1}\ cm^{-1}$). Each trace was repeated 3−5 times to ensure reproducibility. One of either chlorite or Fe(TF_4TMAP) was held constant, while the other was varied in the obtainment of kinetic plots. All concentrations noted here represent post-mixing values. For Fe(TF_4TMAP) dependence, initial [ClO_2^-] was 0.038 M, and Fe(TF_4TMAP) was varied between from 2.5×10^{-5} to 2.5×10^{-4} M. For ClO_2^- dependence, Fe(TF_4TMAP) was 6.2×10^{-6} M, and ClO_2^- was varied from 0.0012 to 0.012 M. These profiles exhibited a sigmoidal shape (see Supporting Information) with an induction period.

The plot in Figure 5C was generated using the instantaneous rate method in the following way: An instantaneous rate under steady state conditions was calculated by fitting a line through the inflection point of the trace (inflection point determined by second derivative method). This rate was divided by the reagent being held constant, $[Fe(TF_4TMAP)]_{Total}$, and the resulting normalized rates were plotted versus the concentration of the reagent being varied (chlorite) at the inflection point. The concentration of chlorite at inflection was determined from the absorbance value at the inflection point.

In addition to the instantaneous rate method, curve fitting was used to analyze the kinetic traces. This analysis leads to the same conclusions as the use of instantaneous rates (see discussion section).

For kinetic measurement using O=Fe^{IV}(TF_4TMAP) (compound II) as the initial form of catalyst, compound II was generated by the addition of 3 equiv of $KHSO_5$ to 6.2×10^{-6} M Fe(TF_4TMAP). This solution was used as catalyst in the decomposition of a 0.012 M solution of chlorite. The resulting plot was similar to those in the absence of HSO_5^- except that the induction period disappeared.

Ion Chromatography on Reaction Products. A typical IC determination is as follows. To 9 mL of a 50 mM solution of $NaClO_2^-$ was added 1 mL of a 4 mM solution of Fe(Por) (each in 50 mM pH 7.14 phosphate buffer) and stirred for 30 min. This solution was diluted 100× and quantified by IC. For ABTS runs, a 10-fold excess of ABTS over chlorite was used in the solution.

Preparation of Isotopically Labeled $NaCl^{18}O_2$. Isotopically labeled chlorite was prepared and used in situ based on a modified protocol for the production of sodium chlorite from sodium chlorate.[37] In a thick-walled Schlenk tube, 2.1 g (20 mmol) $NaClO_3$ was stirred in 5 mL of 95% enriched $H_2{}^{18}O$. To this mixture, 0.83 mL of concentrated sulfuric acid was added, and the mixture was capped and stirred for 1 h at 70 °C. After this period, the tube was removed from heat, cooled to room temperature, and frozen in liquid N_2. The tube was opened to air, and 1.1 g (9 mmol) of solid Na_2SO_3 was added to the frozen mixture. The tube was sealed and warmed to melt the solution, and the mixture was placed back in the heating bath and stirred for 1.5 h in the dark to afford the appearance of yellow ClO_2 gas. This gas was bubbled through an ice-cold solution of NaOH (9 mmol), 1.1 mL of 30% H_2O_2 (9.7 mmol), and 2 mL of H_2O. The resulting solution was stirred with 0.5 g of MnO_2 to disproportionate unreacted H_2O_2 for 2 h and then filtered to remove MnO_2. Analysis of this solution by IC reveals a chlorite concentration of 79.8 ± 0.8 mM, and an approximate 1.5-fold contamination by chloride. Before use in further experiments, the solution was titrated to neutrality with 3 M H_3PO_4 (typically 1−1.5 mL). The resulting solution is 77% ^{18}O-enriched ClO_2^- (based on ESI MS and on the enrichment of resulting O_2 when the compound is dismuted) in phosphate buffer (0.6 M). Further details are available in the Supporting Information.

Chlorite Dismutation - Double Crossover. One milliliter of a mixture of unlabeled chlorite and 18-O chlorite (ca. 75 mM in each) in 0.3 M phosphate buffer, pH = 7.2, was disproportionated by the addition of 0.1 mL of 1 mM Fe(TF_4TMAP). The resulting O_2 was analyzed by RGA mass spectrometer using N_2 as a carrier gas.

Acknowledgment. This work was supported by a grant from the National Science Foundation (CHE-0502391 and 0749572). We gratefully acknowledge Professor Dale Margerum, Dr. Katya Albert, Professor Paul Shepson, and Ms. Chelsea Thompson for their assistance with ion chromatography experiments. We thank Professor Hilkka Kentämaa, Mr. Stephen Habicht, and Dr. Karl Wood for assistance with ESI mass spectrometry. We gratefully acknowledge the efforts of Alan Ronemus for design and implementation of the RGA, as well as for generation of schematics for the instrument published here.

Supporting Information Available: Ion chromatograms, EI mass spectra of O_2 products formed in ^{18}O-water, ESI mass spectra of ClO_3^- products formed in ^{18}O-water, sample kinetic profiles and derivation of complex rate equations via steady state approximation, data on preparation of isotopically enriched $Cl^{18}O_2^-$, and schematic diagram of in-house built RGA (PDF). This material is available free of charge via the Internet at http://pubs.acs.org.

IC801681N

(37) Zhou, C.; Long, J.; Xu, P. *Huaxue Shijie* **1993**, *34*, 38.